Materials Letters 176 (2016) 33–37

Contents lists available at ScienceDirect

Materials Letters

journal homepage: www.elsevier.com/locate/matlet

Single-layer MnO_2 nanosheets: From controllable synthesis to free-standing film for flexible supercapacitors

Ying Yu [a,b], Yunyun Zhai [b], Haiqing Liu [b,*], Lei Li [a,b]

[a] School of Petrochemical Engineering, Changzhou University, 213614 Changzhou, China
[b] College of Biological, Chemical Sciences and Engineering, Jiaxing University, 314001 Jiaxing, China

ARTICLE INFO

Article history:
Received 13 January 2016
Received in revised form
28 March 2016
Accepted 9 April 2016
Available online 11 April 2016

Keywords:
Manganese dioxide
Hybrid film
Flexible supercapacitor
Energy storage and conversion
Nanocomposites

ABSTRACT

Supercapacitors, as one type of significant power source and energy storage unit, have attracted more and more attention. However, designing well-organized electrode structures to endow the flexible supercapacitors with excellent performances still remains a challenge. Here, the ultrathin MnO_2 nanosheets with a thickness of 0.9 nm were produced and used for ideal building blocks of 2D architectures. The free-standing film were prepared by vacuum-assisted filtration and the following mild thermal treatment, which were used directly as a binder-free electrode for flexible supercapacitors. Such unique lamellar structure were favorable for electron transfer from MnO_2 to rGO. As a consequence, a high specific capacitance of 98 F g^{-1} at 50 A g^{-1} is achieved. Remarkably, the capacitance retention after 6000 cycles is more than 95%.

© 2016 Elsevier B.V. All rights reserved.

1. Introduction

Supercapacitors have attracted considerable attention because of the ultrahigh power density, large rate capability and long cycling lifetime [1]. Among them, graphene based materials, such as graphene [2], graphene/CNTs [3] and graphene/MnO_2 [4], have been exploited as active materials by taking advantage of the unique properties of graphene and the synergistic effect between graphene and the other electroactive component. However, the relatively low electrical conductivities of graphene-based films limited their superior performances, because of the presence of defect, and residual oxygen-containing functional groups for chemically exfoliated graphene sheets. Additionally, a larger number of contact resistance between graphene nanosheets and the other nanomaterials also drastically degraded their electrical transport properties. Thus, reasonably designing and preparing the highly conductive and flexible graphene-based films with low cost and facile preparation processes is still a challenge for the high-performance energy storage devices [5,6].

To solve the aforementioned problems, one effective way is to design and build a novel well-organized graphene-based nanostructure combining electrical double layer capacitive and pseudocapacitive. At the same time, accessible electrochemically activated surface area and electrical conductivity of the main components should be improved. In the present work, the MnO_2 and GO nanosheets were used as the model case for the reconstitution toward well-organized films. Benefiting from the synergistic effect of rGO and MnO_2, the MrG hybrid electrode exhibited excellent capacitive performance at high current density.

2. Experimental section

2.1. Materials

Natural graphite flake was purchased from Alfa Aesar. Cellulose acetate membrane (150 nm) was purchased from Toyo Roshi Kaisha, Ltd. (Japan).

2.2. Preparation of graphene oxide (GO) and single-layer MnO_2 nanosheets

The precursor GO was synthesized based on the modified Hummers method [6]. Single-layer MnO_2 nanosheets were synthesized as previous methods [7].

2.3. Preparation of MnO_2-rGO (MrG) hybrid film

As shown in Scheme 1, a homogeneous slurry of MnO_2 and GO with different MnO_2/GO weight ratio (20%, 33%, 50% and 60%)

* Corresponding author.
E-mail addresses: lhq811121@163.com (H. Liu), lei.li@mail.zjxu.edu.cn (L. Li).

http://dx.doi.org/10.1016/j.matlet.2016.04.060
0167-577X/© 2016 Elsevier B.V. All rights reserved.

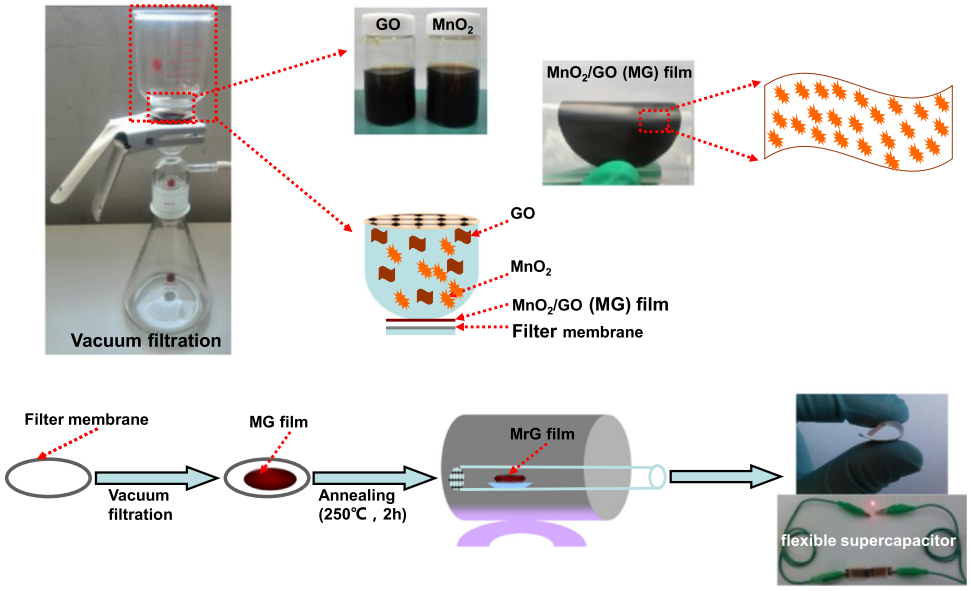

Scheme 1. Illustration of the preparation procedure of MrG membranes.

were mixed and stirred for 0.5 h. Subsequently, the resulting suspensions were vacuum-filtrated. The obtained film was dried at room temperature and annealed at 250 °C for 2 h in N_2 to convert GO to rGO. Based on the different amount of MnO_2, the obtained MnO_2/rGO (20%), MnO_2/rGO (33%), MnO_2/rGO (50%) and MnO_2/rGO (60%) film were named as MrG-1, MrG-2, MrG-3 and MrG-4, respectively.

2.4. Characterization

Scanning electron microscopy (SEM) were performed on an FEI Sirion-200 field emission scanning electron microscope. Transition electron microscopy (TEM) were conducted on a JEOL-2100 electron microscope. Atomic force microscopy (AFM) images were taken with a Nanoscope III (MikroMash, Wislsonville, Oregen).

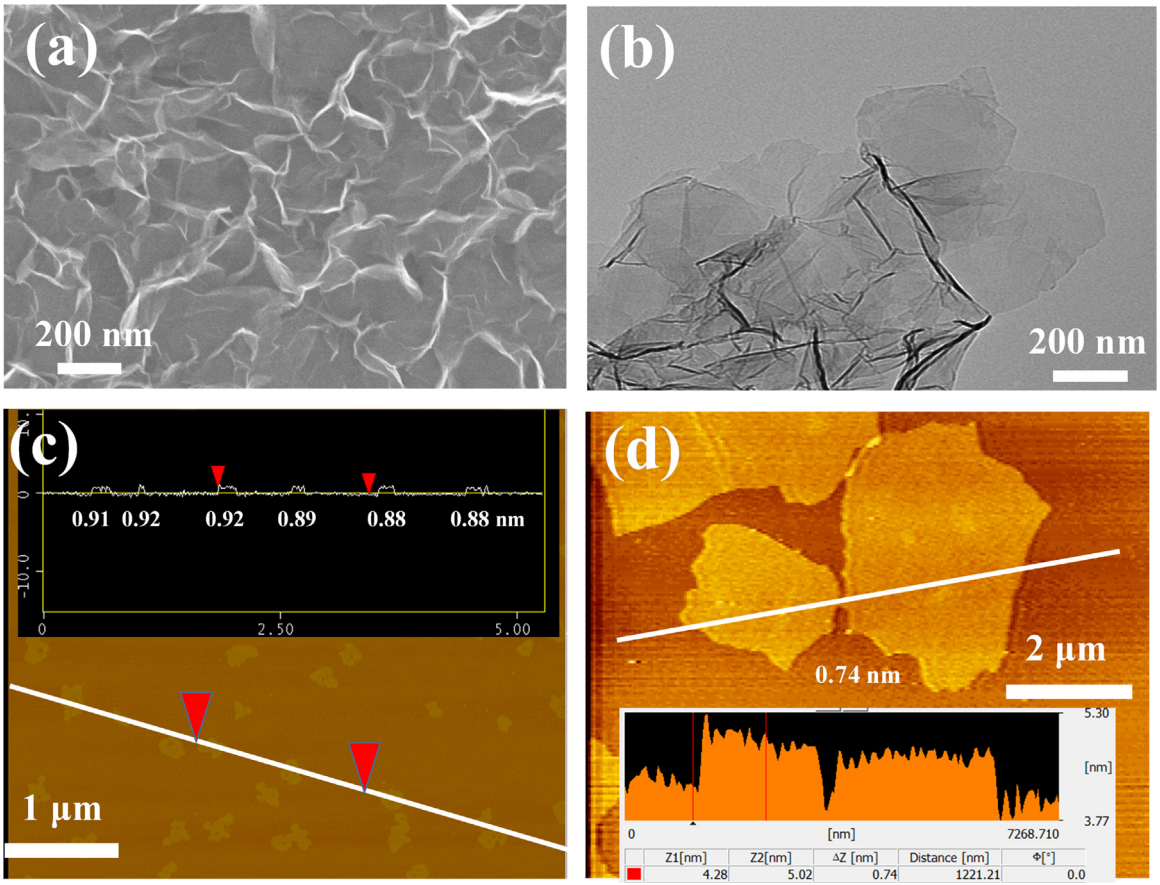

Fig. 1. (a) SEM, (b) TEM and (c) AFM images of MnO_2 nanosheets. (d) AFM image of GO nanosheets.

Raman measurements were recorded on an Invia/Reflrx Lasser Micro-Raman spectroscope (Renishaw, England). X-ray photoelectron spectroscopy (XPS) experiments were carried out on an AXIS Ultra DLD system from Kratos.

All electrochemical tests were carried out using a potentiostat/galvanostat (CHI 660). The electrochemical performances were investigated via a symmetric two electrode supercapacitor system. A neutral aqueous LiCl/PVA was used as an electrolyte for the semi-solid state flexible supercapacitor. The thickness of film was about 20 μm. The area of single film on the electrode was about 0.5 cm^2. The mass of single film on the electrode was about 0.5 mg. Galvanostatic charge/discharge measurements were conducted on a battery tester (Land CA2001A). The specific capacitance(C) of the film electrodes was calculated from the galvanostatic charge-discharge (GCD) curve measured using the equation $C(F/g)=I/(\Delta E/\Delta t)m$, where I is the discharge current (A), ΔE is the potential range of the discharge process (V), Δt is the discharge time (s), and m is the mass of the film electrodes.

3. Results and discussion

A template-free and one-step synthesis of single-layer MnO_2 nanosheets were prepared. As shown in Fig. 1, ultrathin MnO_2 nanosheets with graphene-like wrinkles had been observed, displaying a typical 2D morphology. The average lateral dimension was estimated to be ~200 nm. The nearly transparent feature indicated the ultrathin thickness, which is further verified by the AFM image in Fig. 1(c). The height profile revealed a thickness of approximately 0.9 nm, which illustrates that the nanosheets of MnO_2 is single layer [7]. Based on the ultrathin nanosheets of MnO_2 and GO (single layer, in Fig. 1(d)), the hybrid film was prepared by a facile vacuum filtration of the mixed dispersion of GO and MnO_2 suspension. Then graphene oxide was converted to its reduced form through a thermal reduction.

The nanosheets of MnO_2 contains crystal water and oxygenous group. So the zeta potential of MnO_2 nanosheets solution was negative. The zeta potential of the graphene oxide (GO) was also negative. So the mixed solution of MnO_2 and GO was homogeneous becaused of the electrostatic repulsion. In the vacuum filtration process, the MnO_2 and GO nanosheets precipitate synchronously. So the small MnO_2 nanosheets embedded into the layer of large GO nanosheets. After the thermal reduction and crosslinking, the layer by layer films composed of small MnO_2 nanosheets and large reduced graphene oxide (rGO) were prepared. The morphology of the as-prepared 2D architecture was initially investigated by SEM (Fig. 2). It is important that homogeneous lamellar structure of MnO_2 and rGO was formed. It can be clearly seen from the inset of Fig. 2(a), the MrG-3 (6.0%, 123 MPa) film exhibited approximate mechanical properties in comparison with that of the rGO (6.2%, 140 MPa), which could be helpful for the flexible supercapacitors. From the Fig. 2(c), the crystal form in the MrG maintained. As shown in the XPS spectra of Fig. 2(d), the intense peak at 648 cm^{-1} was assigned to Mn-O vibration mode [7]. The two peaks at 1342 and 1588 cm^{-1} can be assigned to d-and G-bands of rGO, respectively. Surface chemical analysis of the MrG films was performed using XPS. As shown in Fig. 2(e), XPS of Mn displayed two peaks centered at 640.8 and 653.3 eV, corresponding to $Mn_{2p3/2}$ and $Mn_{2p1/2}$ of MnO_2, respectively. It is noteworthy that the signal for O 1s showed single peak (530.3 eV), which represented the oxygen in the lattice of [MnO_6] octahedral. After annealing at 250 °C, the deconvolution of C 1 s peak still

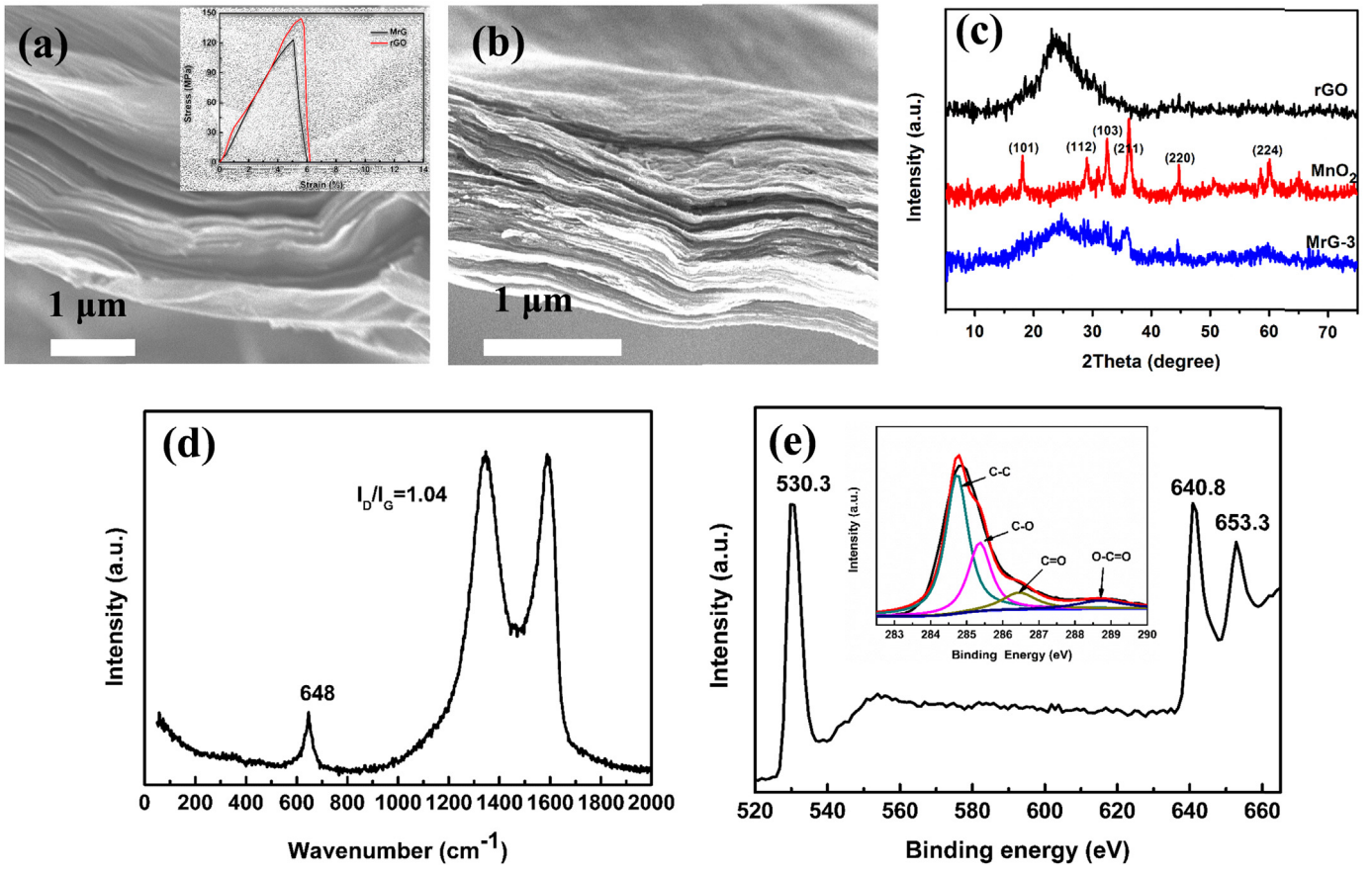

Fig. 2. Cross-sectional images of the (a) rGO and (b) MrG-3 films. Inset of 2(a) was the stress–strain curves of relevant films. (c) XRD of rGO, MnO_2 and MrG-3. (d) Raman and (e) XPS spectrum of MrG-3 film.

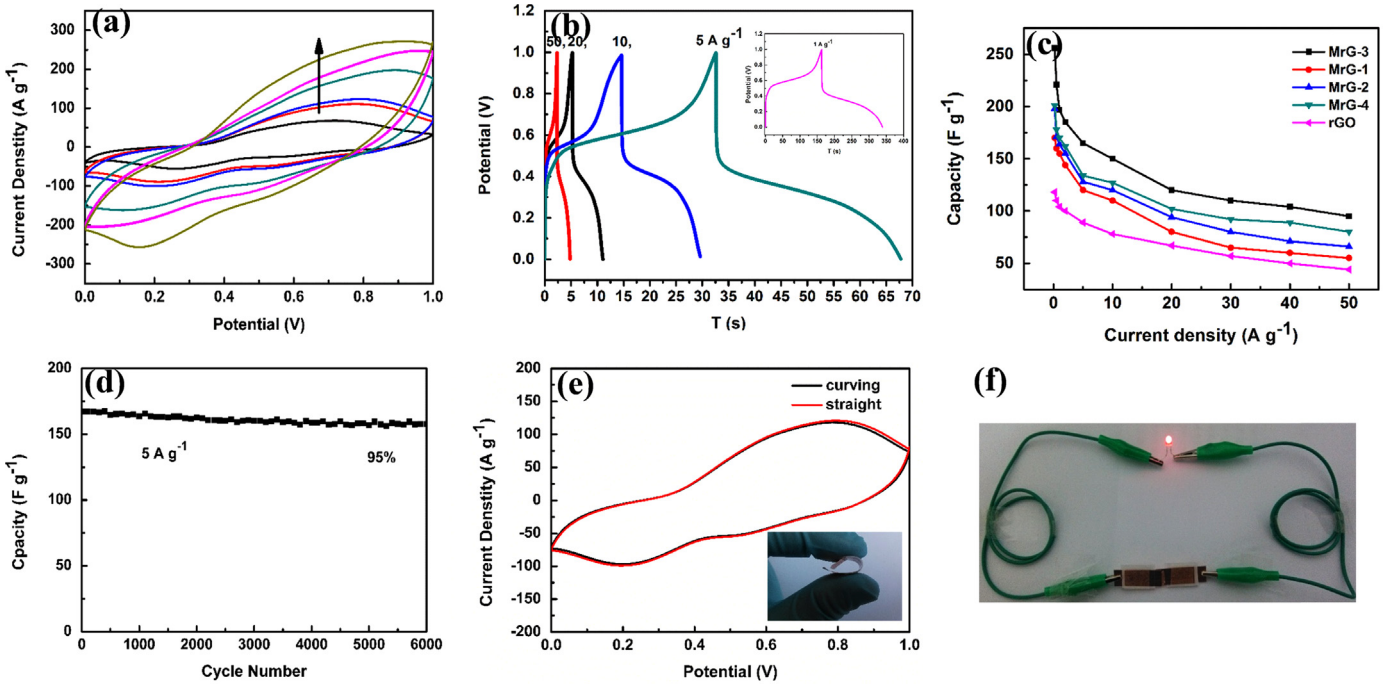

Fig. 3. (a) CV curves of MrG-3 films at different scan rate of 50, 80, 100, 300, 500 and 800 mV s^{-1}. (b) Charge/discharge curves of MrG-3 at five current densities. (c) Current density dependence of specific capacitance for MrG-1, MrG-2, MrG-3 and MrG-4. (d) Cycling performance of MrG-3. (e) CV curves of the flexible supercapacitor on straight and curving states at 5 A g^{-1}. (f) A light-emitting diode (LED) powered by 2 supercapacitors in series.

revealed three characteristic peaks corresponding to C-O, C=O, and O-C=O, indicating the presence of oxygenated functional groups on the rGO. Although annealing at this temperature showed no complete remove of the oxygenated functional groups, the flexibility and mechanical strength of MrG films were well maintained.

The electrochemical properties were investigated using cyclic voltammetry (CV) and GCD measurements. As shown in Fig. 3(a), the CV curves show a quasi-reversible oxidative and reductive shape, indicating a good reversibility of 2D MrG films architecture for energy storage. The specific capacitance (C, in F g^{-1}) of the electrode was calculated by an equation $C=(\int IdV)/(2mvV)$, where I is the response current, ν is the scan rate, m is the mass of active material, and V is the scan potential window used in a two-electrode cell. At a scan rate of 100 mV s^{-1}, the specific capacitance of MrG-3 film was as high as 232 F g^{-1}, showing high-rate storage capability. The charge/discharge curves for different currents of MrG-3 film in Fig. 3 (b) indicated that the high capacitance of MrG-3 film was maintained at high current densities (from 5 to 50 A g^{-1}) [8]. The capacitance of MrG films also depend on the weight ratio of MnO_2 to GO. The specific capacitances of the MrG films increased with increasing MnO_2 ratio from 20% to 50%. At the current density of 5 A g^{-1}, the MrG-3film exhibited a significantly higher specific capacitance (163 F g^{-1}) compared to that of MrG-1 (117 F g^{-1}) and MrG-2 (130 F g^{-1}) films. This difference can be attributed to the pseudocapacitance effect of MnO_2 in the thin film electrode. While when the ratio increased from 50% to 60%, the capacitances were decreased because of the poor electrical conductivity of MnO_2 in contrast with rGO. Within the whole current density range, the MrG-3 yielded substantially higher specific capacitance than that of the other samples. The specific capacitance can be still maintained as high as 98 F g^{-1} at a very fast charge-discharge rate of 50 A g^{-1}. It was 1.98, 1.51 and 1.21 times higher than that of MrG-1 (53 F g^{-1}), MrG-2 (65 F g^{-1}) and MrG-4 (81 F g^{-1}), respectively.

Cycling capability is an important requirement for supercapacitor applications, which largely restricts the energy storage performance [9]. The cycling life tests over MrG film electrodes for 6000 cycles at a current density of 5 A g^{-1} were carried out using charge/discharge technique (Fig. 3(d)). Inspiringly in this work, after introducing large rGO sheets to the interlamination of MnO_2, a largely enhanced cycling stability was obtained. The results further verified the great potentiality of MrG nanocomposite as efficient supercapacitor material with high specific capacitance and good cycling stability. The effect of curvature on the device performance was examined by CV behavior at bending state. As shown in Fig. 3(e), no apparent change was observed, revealing a satisfactory electrochemical performance even under the bending conditions (180°). As shown in Fig. 3(f), the assembled symmetrical flexible supercapacitor with excellent flexibility and well mechanical properties for LED test, can undergo severe blending.

4. Conclusion

We have demonstrated that the flexible MrG nanocomposite films can be prepared and used as the electrode of a flexible supercapacitor without any other organic binders and conductive agent. These MrG films were very stable under repeated charging/discharging, delivering over 95% of the initial capacitance after 6000 cycles. All these attractive features make this class of flexible MrG film materials promising for large-scale real-world applications.

Acknowledgements

This work was supported by the National Natural Science Foundation of China (Nos. 21177049, 51503079 and 51103063).

References

[1] Y. He, W. Chen, X. Li, Z. Zhang, J. Fu, C. Zhao, E. Xie, ACS Nano 7 (2013) 174.
[2] (a) X. Zhao, C.M. Hayner, M.C. Kung, H.H. Kung, ACS Nano 5 (2011) 8739;
(b) Z. Xiong, C. Liao, W. Han, X. Wang, Adv. Mater. 27 (2015) 4469.

[3] P. Duy Tho, T.H. Lee, D.H. Luong, F. Yao, A. Ghosh, L. Viet Thong, T.H. Kim, B. Li, J. Chang, Y.H. Lee, ACS Nano 9 (2015) 2018.
[4] Z. Li, Y. Mi, X. Liu, S. Liu, S. Yang, J. Wang, J. Mater. Chem. 21 (2011) 14706.
[5] K. Yuan, Y. Xu, J. Uihlein, G. Brunklaus, L. Shi, R. Heiderhoff, M. Que, M. Forster, T. Chasse, T. Pichler, T. Riedl, Y. Chen, U. Scherf, Adv. Mater. 27 (2015) 6714.
[6] X. Yang, C. Cheng, Y. Wang, L. Qiu, D. Li, Science 341 (2013) 534.
[7] Z. Liu, K. Xu, H. Sun, S. Yin, Small 11 (2015) 2182.
[8] (a) Y. Zeng, Y. Han, Y. Zhao, Y. Zeng, M. Yu, Y. Liu, H. Tang, Y. Tong, X. Lu, Adv. Energy Mater. (2015) 5;
(b) D. Yu, S. Zhai, W. Jiang, K. Goh, L. Wei, X. Chen, R. Jiang, Y. Chen, Adv. Mater. 27 (2015) 4895.
[9] J.-X. Feng, S.-H. Ye, A.-L. Wang, X.-F. Lu, Y.-X. Tong, G.-R. Li, Adv. Funct. Mater. 24 (2014) 7093.